

# UWB Indoor Radio Propagation Modelling in Presence of Human Body Shadowing Using Ray Tracing Technique

Rachid Saadane, Mohammed Wahbi

SIR2C2S/LASI-EHTP, Electrical Engineering  
Department Ecole Hassania des Travaux Publiques, Casablanca Maroc  
rachid.saadane@gmail.com

**Abstract:** This paper presents a ray-tracing method for modeling Ultra Wide Bandwidth indoor propagation channels. A validation of the ray tracing model with our indoor measurement is also presented. Based on the validated model, the multipath channel parameter like the fading statistics and root mean square  $T_{rms}$  delay spread for Ultra Wide bandwidth frequencies are simply extracted. The proposed ray-tracing method is based on image method. This is used to predict the propagation of UWB electromagnetic waves. First, we have obtained that the fading statistics can be well fitted by log normal distribution in static case. Second, as in realistic environment we cannot neglect the significant impact of Human Body Shadowing and other objects in motion on indoor UWB propagation channel. Hence, our proposed model allows a simulation of propagation in a dynamic indoor environment. Results of the simulation show that this tool gives results in agreement with those reported in the literature. Specially, the effects of people motion on temporal channel properties. Other features of this approach also are outlined.

**Keywords:** Ray tracing, Delay spread, UWB Indoor propagation, Human Body.

## 1. Introduction

Ultra wideband (UWB) technology has appeared as one of the most promising candidates for many indoor communication applications like security systems, wireless personal area network, wireless home networking, ... Exact channel characterization is essential for UWB transceiver design. Given the wideband nature of UWB signals, that is, up to 10 of GHz of frequency bandwidth the conventional channel models developed for narrowband transmissions are inadequate for UWB transmission. The basic difference between a narrowband and UWB multipath model is that in the UWB model each path will have its own IR or frequency transfer characteristics that is frequency dependent. Therefore, there is a need to consider UWB signal distortion, which will depend on the UWB channel propagation model [7].

The people interest of UWB technology is for very different purposes such high speed, short range networking in support of a variety of potential low cost, low power multimedia transport application in home and enterprise environments. Such techniques, as well as others are being considered in the standardization process of the IEEE 802.15.3a Wireless Personal Area Network (WPAN) proposal [8]. At the same time, regulatory aspects are quickly being defined by the Federal Communications Commission (FCC).

The well known experimental and simulation techniques can be used to investigate the propagation UWB signals in indoor environments. In this paper the simulation one is developed, used and compared with experimental approach.

The advantage of experimental method is that all system and channel parameters affecting the propagation UWB signals are accounted for without pre-assumptions. But this method is usually luxurious, time consuming, and limited by the characteristics of available equipment. On the other hand, simulation techniques are free from the limitations of experimental approaches but they require more computational time. They also need sophisticated computational resources to carried out simulations.

In this paper, in first time, we compare the channel parameters based on the RT model with in-indoor collected measurements [2], [5], [6]. Subsequently, we provide results for the fading statistics of the received power and the root mean square (RMS) delay spread for an UWB indoor propagation channels.

After the validation of the proposed method, in second time, we studied the channel parameters within people in motion based on the RT model [1]. Subsequently, we provide results for the fading statistics of the received power with persons in motion.

The remainder of this paper is organized as follows. The UWB channel characterization using ray tracing in the literature and physical models are presented in Section IV. In Section V we present briefly the simulation set-up and we draw results. In section X we present some conclusions of this study.

## 2. Physical Models And Ray Tracing For Uwb

### A. Ray tracing and UWB channel modelling:

In the last decay the deterministic solution of Maxwell's equations using high-frequency approximations, this method recall ray tracing, has become widely used tool for channel simulation, characterization, prediction and network planning and optimization. Traditional ray tracing or ray launching follows rays on their path from transmitter to receiver. Since UWB systems do not fulfil the narrowband assumption, this principle obviously needs to be modified for UWB simulations. One possible approach performs traditional ray tracing at different frequencies, and then combines the results. An alternative computes the impulse responses of the different rays (which depends on the communication processes they go through) and adds up the contributions from the different rays [27], [29], [30] used a mixture of ray tracing with FDTD. Refs. [31] and [32] have independently

suggested a to combine deterministic components that are derived from ray tracing.

With a Rayleigh-distributed "clutter" that describes the contributions that stem from diffuse scattering and other propagation paths that are not covered by the ray tracing. For outdoor LOS environments [31], two deterministic components (direct wave and ground wave) are often sufficient, while for indoor environments, [32] have suggested the use of up to three reflections.

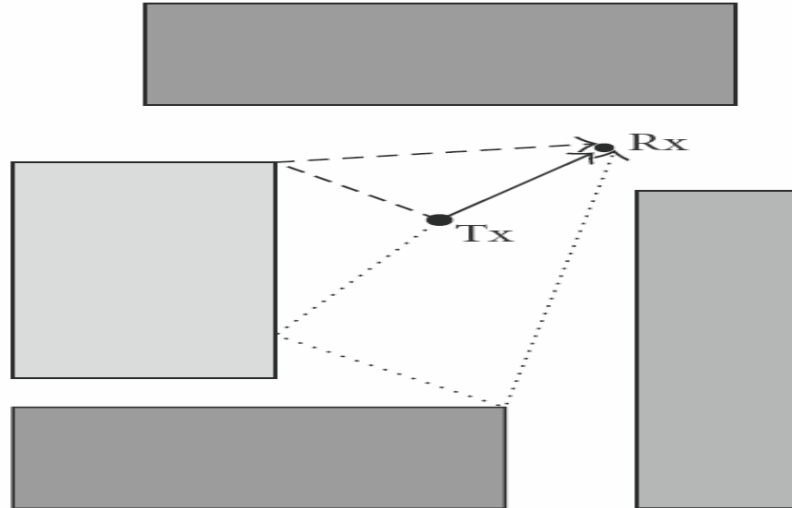


**Figure 1.** Simple RT illustration: propagation scenario (gray shading indicates buildings).

and the corresponding propagation process can be simulated using computer programs. Deterministic models are physically meaningful, and potentially accurate. However, they are only representative for the environment considered. Hence, in many cases, multiple runs using different environments are required. Due to the high accuracy and adherence to the actual propagation process, deterministic models may be used to replace measurements when time is not sufficient to set up a measurement campaign or when particular cases, which are difficult to measure in the real world, will be studied. Although electromagnetic models such as the method of moments or the finite difference in time domain model may be useful to study near field problems in the vicinity of the Tx or Rx antennas, the most appropriate physical deterministic models for radio propagation, at least in indoor areas, are ray tracing (RT) models. RT models use the theory of geometrical optics to treat reflection and transmission on plane surfaces and diffraction on rectilinear edges [23]. Geometrical optics is based on the so-called ray approximation, which assumes that the wavelength is sufficiently small compared to the dimensions of the obstacles in the environment. This assumption is usually valid in urban radio propagation and allows to express the electromagnetic field in terms of a set of rays, each one of them corresponding to a piecewise linear path connecting two terminals. Each "corner" in a path corresponds to an "interaction" with an obstacle (e.g., wall reflection, edge diffraction). Rays have a null transverse dimension and therefore can in principle describe the field with infinite resolution. If beams (tubes of flux) with a finite transverse dimension are used instead of rays, then the resulting model is called beam launching, or ray splitting. Beam launching models allow faster field strength prediction but are less accurate in characterizing the radio channel between two SISO or MIMO terminals [26]. Therefore, only RT models will be described in further detail here.

### B. Physical models

Physical propagation models are named «deterministic» if they aim at reproducing the actual physical radio propagation process for a given environment. In indoor environments, laboratories, home and industrial environments, the geometric and electromagnetic properties, characteristics, of the environment and of the radio channel can be stored in files

### C. RT Algorithm

With RT algorithms, initially the Tx and Rx positions are specified and then all possible paths (rays) from the Tx to the Rx are determined according to geometric considerations and the rules of geometrical optics. Usually, a maximum number  $N_{max}$  of successive reflections/diffractions (often called prediction order) is prescribed. This geometric "ray tracing" core is by far the most critical and time consuming part of the RT procedure. In general, one adopts a strategy that captures the individual propagation paths via a so-called visibility tree Fig. 2. The visibility tree consists of nodes and branches and has a layered structure. Each node of the tree represents an object of the scenario (a building wall, a wedge, the Rx antenna, dots) whereas each branch represents a line-of-sight (LoS) connection between two nodes/objects. The root node corresponds to the Tx antenna. The visibility tree is constructed in a recursive manner, starting from the root of the tree (the Tx). The nodes in the first layer correspond to all objects for which there is an LoS to the Tx. In general, two nodes in subsequent layers are connected by a branch if there is LoS between the corresponding physical objects.

This procedure is repeated until layer  $N_{max}$  (prediction order) is reached. Whenever the Rx is contained in a layer, the corresponding branch is terminated with a "leaf." The total number of leaves in the tree corresponds to the number of paths identified by the RT procedure. The creation of the visibility tree may be highly computationally complex.

Once the visibility tree is built, a backtracking procedure determines the path of each ray by starting from the corresponding leaf, traversing the tree upwards to the root node, and applying the appropriate geometrical optics rules at each traversed node. To the  $i$ th ray, a complex, vectorial electric field amplitude  $E_i$  is associated, which is computed by taking into account the Tx-emitted field, free space path

loss, and the reflections, diffractions, and so forth experienced by the ray. Reflections are accounted for by applying the Fresnel reflection coefficients [33], whereas for diffractions the field vector is multiplied by appropriate diffraction coefficients obtained from the uniform

geometrical theory of diffraction. The distance-decay law (divergence factor) may vary along the way due to diffraction. The resulting field vector at the Rx position is composed of the fields for each of the  $N_r$  rays.

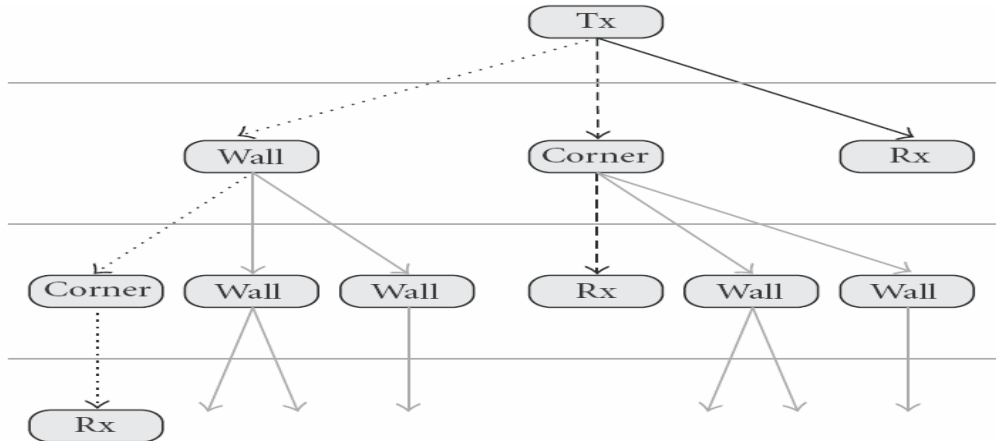


**Figure 2.** Simple RT illustration: corresponding visibility tree (first three layers shown).

### 3. Measurements

#### A. The Measurement Environment

The Data channel measurements processed in this work were collected during 2003- 2006 in the building of Mobile Communication Laboratory at Eurecom Institute (Sophia anti polis) [5], two were conventional laboratory building built during the 1990s. Measurements are performed at spatially different locations for both Line-Of Sight (LOS) and Non Line Of Sight (NLOS). The experiment area is set by fixing the transmitting antenna on a mast at 1 m above the ground on horizontal linear grid (20 cm) close to VNA and moving the receiver antenna to different locations on horizontal linear grid (50 cm) in 1 cm steps. The height of receiver antenna was also 1 m above the ground. This configuration targets peer-to-peer applications. For one scenario we sorted 3 -50 different complex frequency responses. We repeat the same experiment for various separations between transmitter and receiving antennas varying from 1 meter to 12 meters. Among all positions, we considered both LOS and NLOS configurations.

Measurements were carried out in Eurecom's Mobile Communication Laboratory, which has a typical laboratory

environment (radio frequency equipment, computers, tables, chairs, metallic cupboard, glass windows,...) with plenty of reflective and diffractive objects, rich in reflective and diffractive objects.

For the NLOS case, a metallic plate is positioned between the transmitter and the receiver. In all of the measurements, the channel was kept stationary while the transfer function  $H(f)$  was measured in the sense that no significant movement occurred during a single sweep of frequencies except that required to operate the test equipment. Then, to average out fading, the receiver and transmitter antennas were slightly varied over position for each given separation distance between the two antennas. Thus, for each separation distance a set of measurements were taken, where one measurement is defined as being the response from a single sweep over frequency of the network analyzer. All this measurement are realized over 6 GHz of bandwidth, for all locations both the transmitter and receive antennas remained fixed at equal heights (1.5 meters). Fig. 3 shows the general architectural of the room where the used measurements data in this work are token. From this figure we see that the transmitter position is indicated by Tx and the receiver path is indicated by Rx.

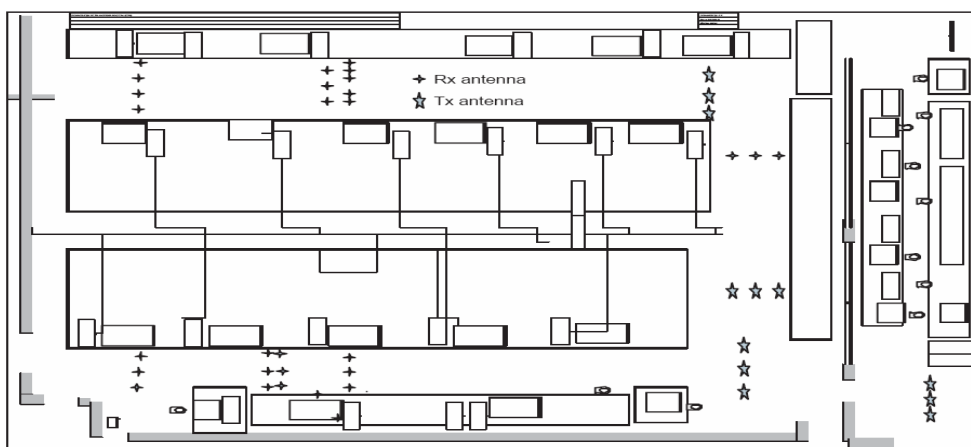


**Figure 3.** Layout of one location where the channel measurements are conducted. The general architectural of the room where the used measurements data are token.

### B. Equipment

The measurement setup was based on ZVM Vector Network Analyzers (Rohde & Schwarz from 10 MHz to 20 GHz), connected to two small and compact, linear phase across frequency and Azimuth Omni-directional antennas with suitable cables. Measurements were swept over the 3 - 9 GHz range, with a frequency resolution of 1 MHz (2001 point per sweep) [5]. The antennas were placed on carts that were moved

to different locations for different measurements, and were immobile during each measurement. A computer controlled the parameters of the network analyzer and the data collection.

## 4. Physical Models And Ray Tracing For Uwb

### A. Ray tracing and UWB channel modelling

In the last decay the deterministic solution of Maxwell's equations using high-frequency approximations, this method recall ray tracing, has become widely used tool for channel simulation, characterization, prediction and network planning and optimization. Traditional ray tracing or ray launching follows rays on their path from transmitter to receiver. Since UWB systems do not fulfill the narrowband assumption, this principle obviously needs to be modified for UWB simulations.

One possible approach performs traditional ray tracing at different frequencies, and then combines the results. An alternative computes the impulse responses of the different rays (which depends on the interaction processes they go through) and adds up the contributions from the different rays [27], [29], [30] used a combination of ray tracing with FDTD. Refs. [31] and [32] have independently suggested a to combine deterministic components that are derived from ray tracing. With a Rayleigh-distributed "clutter" that describes the contributions that stem from diffuse scattering and other propagation paths that are not covered by the ray tracing.

For outdoor LOS environments [31], two deterministic components (direct wave and ground wave) are often sufficient, while for indoor environments, [32] have suggested the use of up to three reflections.

## 5. Simulation Method And Set-Up

For simulation of the UWB propagation we applied ray tracing that we have developed. Next to the indoor wall structure, four metal cabinets and a concrete pillar have been taken into account. The dimensions and locations of these

**Table 1.** Global Parameters Of The Model

Frequency	6 GHz
Antennas	Omnidirectionnel
Polarization	Vertical
High of antennas	1.2 m
Radiated power	0 dBm
Reflection order	5
Transmission	Active
Diffraction order	2
Threshold (minimum level)	-150 dBm

objects are comparable with those can be found in laboratories environment. Complex impulse responses have been generated

up to a maximum delay of 200 ns. The maximum numbers of reflections, diffractions and penetrations were 4, 5 and 6, respectively. The applied antenna radiation patterns were based on measured antenna diagrams [25]. As known the permittivity and conductivity of concrete are two parameters frequency dependent for frequencies beyond 10 GHz. Hence, these parameters are considered as input of our developed tool. Since the dielectric permittivity and the loss tangent of the materials changes with frequency, the different values of dielectric constant and loss tangent of materials for different frequency are carefully considered in channel calculation [21]. The dielectric constant and loss tangent of wood are shown in Table I in [22]. The global parameters of the model are summarized on table I. The Fig. 4 shows the environment in which we have conducted our simulations.



**Figure 4.** Layout of our proposed tool.

### 6. Simulation And Measurement Results For Validation

#### A. Measured channel magnitude and time delay spread

Figs. 5 and 6 show the channel magnitude and the time delay spread for LOS and NLOS cases. From the First figure we observe that the UWB channel characterized by reflections and diffraction. Also, based on the second figure we can

return the normal distribution as best fit to the delay spread parameters in the two cases LOS and NLOS.

#### B. Simulation using RTT approach

The simulation it experienced using our proposed model and with respect to real environment parameters like  $\epsilon_r$ ,  $\sigma$ , channel band and the other parameters. Fig. 7 (a) and (b) present the Power delay profile of channel based on simulation for LOS and NLOS.

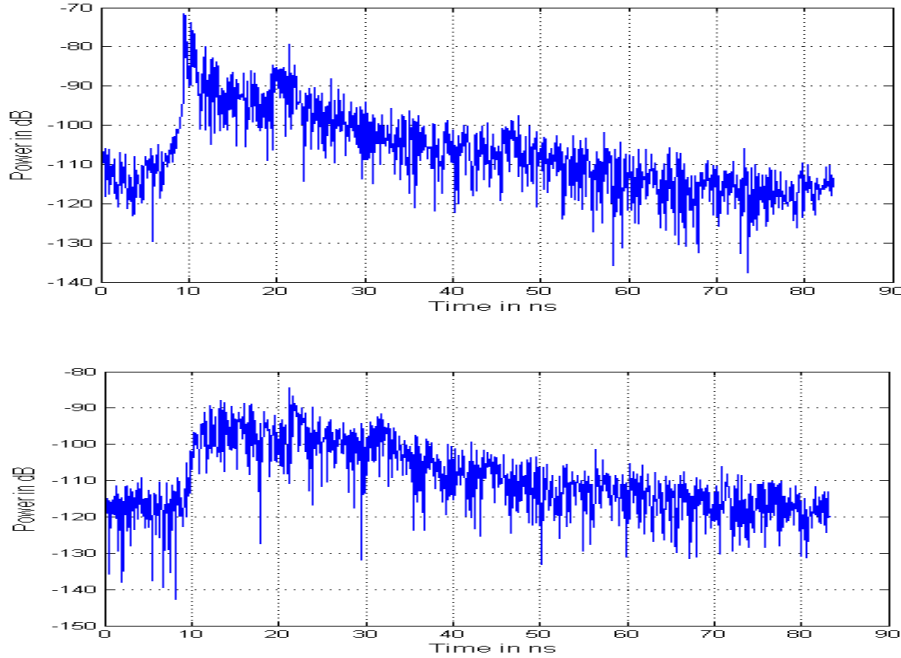


Figure 5. Typical measured channel response impulse LOS and NLOS cases.

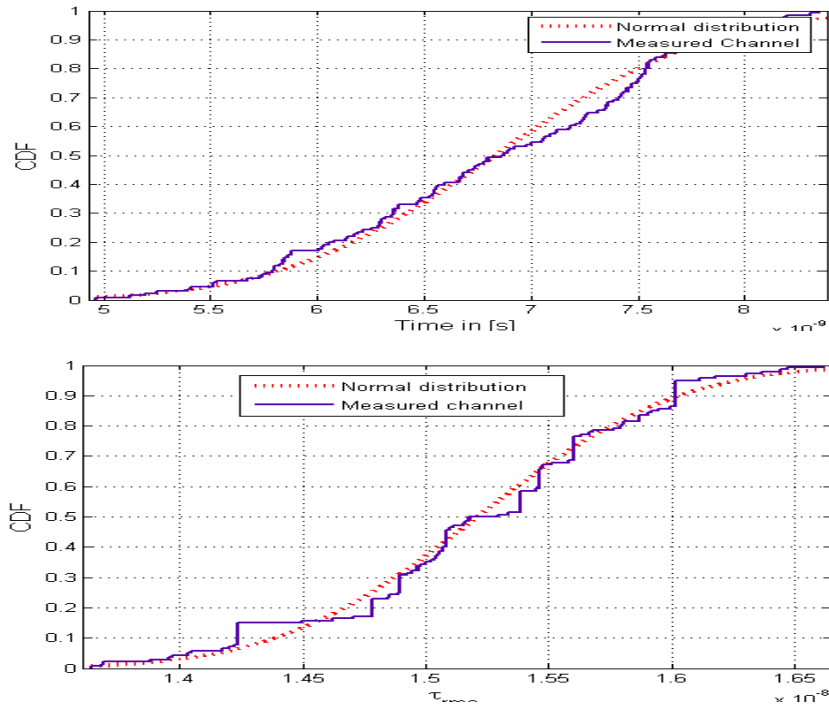


Figure 6. The cumulative distribution function of  $\tau_{RMS}$  from measurement for LOS and NLOS.

From this figure we can observe that the simulated channel is in agreement with measured one based on  $\tau_{RMS}$  values and the clusters profile form.

Fig. 8 illustrates a comparison between the CDF of received signal based on measurement and simulation for two cases LOS and NLOS. The figure shows some similarity not perfect but with a tolerated deviation this because we can not performed the real environment. Thus, the difference

between the received signal for both LOS and NLOS is 6 dB and 6.5 dB.

Some differences can be observed these differences are presumably due to a not perfect reconstruction of the scenario in terms of furniture and dielectric properties of the materials.

Indeed, it can be shown that the RT derived PDP is sensitive to these scenario features, while it is robust towards

the reconstruction of the scenario in terms of its dimensions. Finally, we should point out that, in order to compare the RT results with measurements, some Additive White Gaussian Noise (AWGN) has been added to the individual RT-generated impulse response before using them to get the PDP.

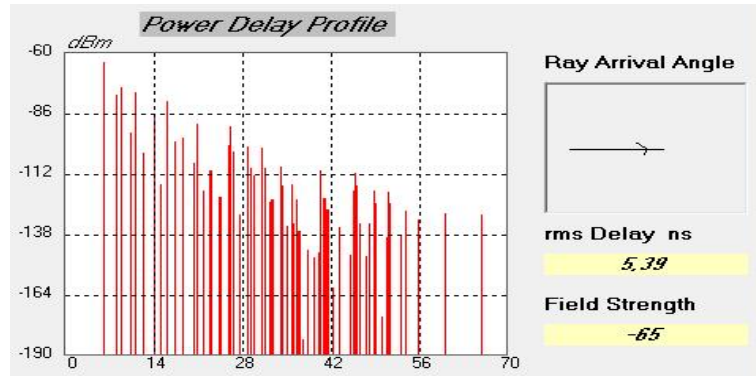


Figure 7. (a) Delay Profile of simulated channel for LOS and NLOS. The label of x axis is the delay in [ns].

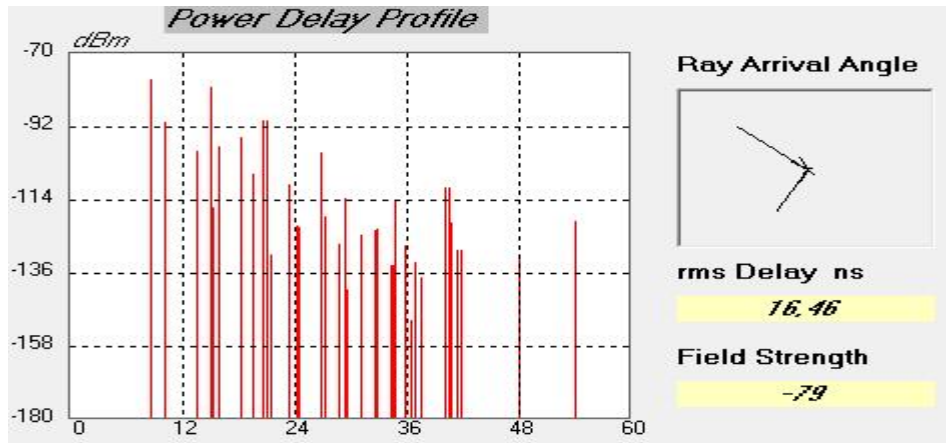


Figure 7. (b) Delay Profile of simulated channel for LOS and NLOS. The label of x axis is the delay in [ns].

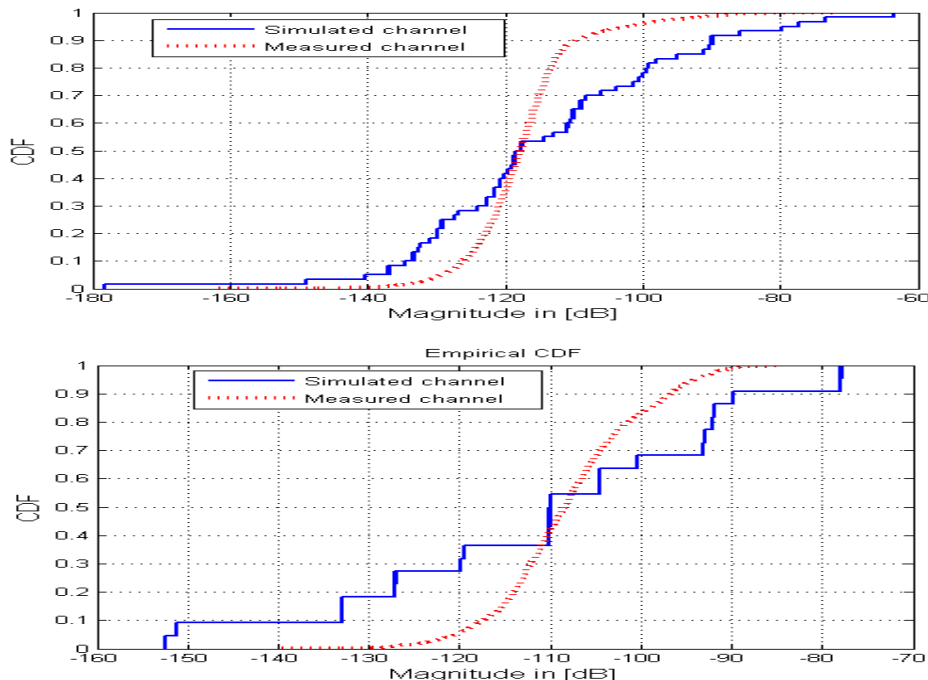


Figure 8. CDF of Magnitude for measured and simulated channels for LOS and NLOS cases.

## 7. Channel Parameters And Fading Model

Subsequently, we carry on pulling out the multipath channel parameter (i.e., RMS delay spread  $\tau_{RMS}$ ) for an UWB indoor.

From simulations we have found that depending of the distance between the Tx and Rx the value of  $\tau_{RMS}$  varies from 2.36 ns to 15 ns. The simulated delay spreads are in

agreement with the measurement results [5]. This also involves that the ray tracing method can be used to calculate the multipath channel parameters at UWB frequencies.

As is well known, indoor propagation involves interactions among furniture, walls, or other objects. Because of these multipath, signals arrive at the receiver with different phases,

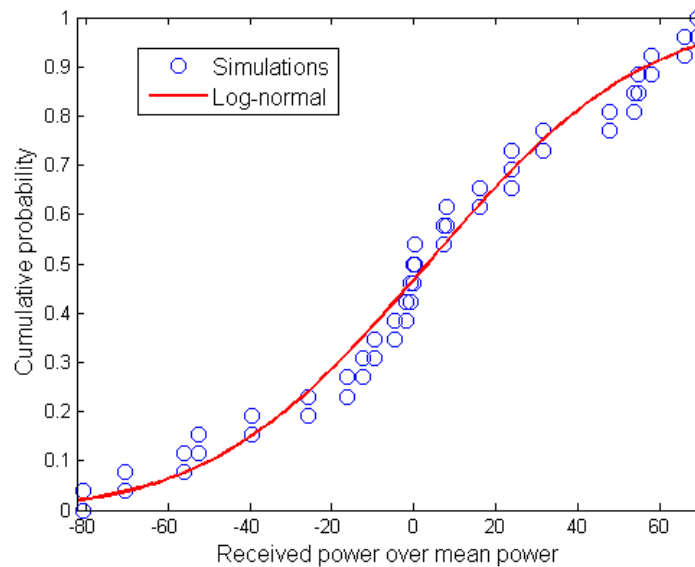


**Figure 9.** Cumulative distributive function (CDF) computed from the received power over mean power. The dots are CDF of the simulations of received power over mean power at environment in which we have conducted simulations, and the depicted solid lines come from the best-fitted Normal distribution.

causing fading. This fading can be obtained statistically from the PDPs by first developing a cumulative distributive function (CDF) based on the probability of receiving energies above a predetermined threshold level. Next, we look for the best-fit distribution for the observed CDF (by means of maximum likelihood estimation). In this analysis, we chose the lognormal

distribution (which has also been used for ultrawideband indoor propagation [35]) for fitting the data. The Normal probability density function can be given by the following.

A variable  $X$  is log-normally distributed if  $Y = \log(X)$  is normally distributed with  $\log$  denoting the natural logarithm. The general formula for the probability density function of the log-normal distribution is

$$f(x|\theta, \sigma) = \frac{1}{(\sigma\sqrt{2\pi(x-\theta)})} \exp\left(-\frac{[\ln(x-\theta)]^2/(2\sigma^2)}{2\sigma^2}\right), x \geq \theta; \sigma, m > 0. \quad (1)$$

where  $\sigma$  is the shape parameter,  $\theta$  is the location parameter and  $m$  is the scale parameter. The case where  $\theta = 0$  and  $m = 1$  is called the **standard log-normal distribution**.

## 8. Dynamic Environment Of Propagation modeling

The objective of this part is to present the human body model that will be supported by the ray tracing technique. This integration of motion aspects in the ray tracing permits to characterize the propagation in realistic environments. Of course, this can be support different millimeter bands (e.g. 17 GHz, 60 GHz and 94 GHz). In this work, the 60 GHz band is investigated and studied.

### A. Human body modeling

In literature, the human body is modeled physically by cylinders containing salty water. Figure 4 in [28] presents the

**Table 2.** Permittivity And Conductivity Versus Frequency

Frequency MHz	Permittivity	Conductivity
100	77	0.70
200	77	0.71
400	76.9	0.73
800	76.8	0.83
1600	76.5	1.22
3000	75.3	2.50

well known models. The model says SALTY supposes the cylinder to contain a solution of salty water with a concentration of 1.5 g/L; the cylinder has a 1.7 m height and a diameter of 0.305 m. The second one called Salty-Lite presented in supposes that the solution in partition having a thickness of 0.04 m, the height of the cylinder is 1.32 m and the diameter is identical to the first model. Figure 5 in [28] presents for a fixed salty water concentration the behavior of complexes permittivity  $\epsilon_r$  versus frequency (In this case the concentration is 1.5 g/L).

Table II summarizes some practical values of the permittivity and conductivity used in to simulate the human body model.

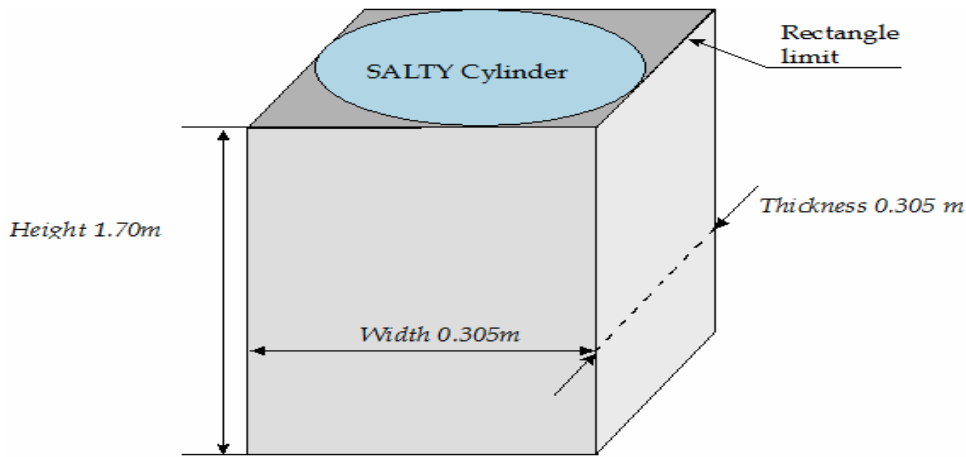


Figure 10. Human body Model.

**B. New model**

For the new model we have used the salty model to simulate the temporal variations of the channel. Unfortunately, ray tracing deals only with plane surfaces, but we can always use a parallelepiped modelling of the human body, i.e. we model the human body by a parallelepiped circumscribed with SALTY cylinder model as depicted on Fig. 10. This figure presents also the geometrical features of the model.

The persons moving near mobile radio link are modeled by objects having a finished dimensions with a parallelepiped form, and, characterized by a permittivity  $\epsilon_r$  a conductivity  $\sigma$ . The model assigns to each object a position which will be modified according to the speed and the direction.

**9. Simulation Set Up And Results**

**A. Simulation setting**

To implement the model described above, we consider a room of dimension 10 m \_20 m many persons randomness

moving (we change the number voluntarily) near around radio link at 6 GHz band. The starting positions of the people are random, speeds are supposed to be constant equal to 0:5 m/s. The positions of transmitter and receiver are indicated on Fig.11 and remain fixed during simulation. The model representing an abject modelling the human body like a wall with two identical facets, these two facets can reflect wave emitted by Transmitter as they can refract and transmit it, but for 6 GHz band there no transmission effect for the human body in our proposed model. The series of simulations are obtained by an automatic change of the positions of the objects modeling the people moving, by respecting their speed of movement and their direction. Simulations are taken with regular time interval, which makes it possible to compute again the positions of the objects and to make a new calculation of the parameters of the channel.

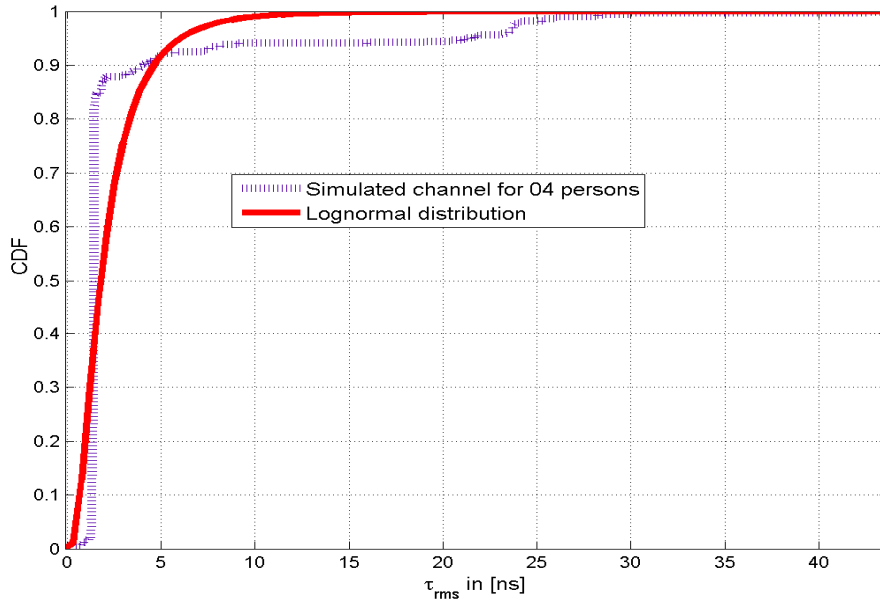


Figure 11. Environment with 20 persons.

**B. Simulation results**

The Fig. 12 presents the distribution of  $\tau_{rms}$  for 04 persons based on simulation and theoretical distribution comparison. Fig. 13 shows the results of 60 seconds of simulation and for 04 persons and distance transmitter/receiver of 08.0015 m.

This figure shows fast fading and variations around an average value of -66.9298 dB. The maximum depth of fading is of -33.8635 dB for 04 persons. Table III presents the max and min values for different number of persons.



**Figure 12.** UWB signals CDF of for 04 bodies in environment and theoretical distributions.

Figs. 14 and 15 show comparison of the impact of number of persons on channel quality. This for relative signal magnitude and  $\tau_{rms}$  respectively.

The UWB channel simulations with bodies on motion around a fixed Tx and Rx antennas allow as to observe an important attenuation of the direct paths in the impulse response. In the case of many persons the attenuation corresponds to the sum of individual attenuation caused by individual persons.

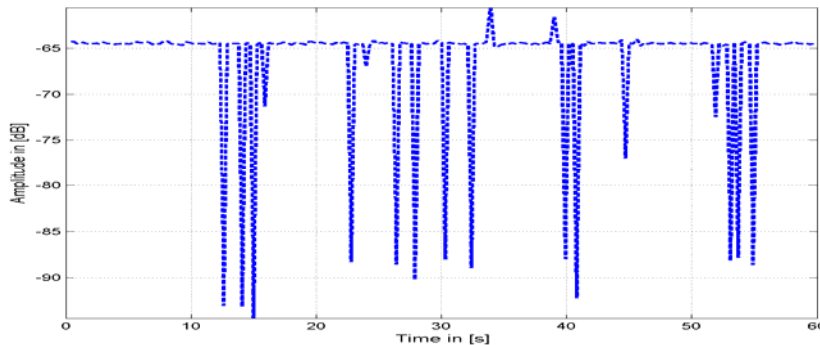


**Figure 13.** Amplitude variations for 04 persons.

Table 3. Maximal And Minimal Values Of The Magnitude For Different

Number of persons	Min in dB	Max in dB
03	-96.7012	-57.3209
04	-94.4413	-58.505778
10	-115.4745	-58.70031
20	-116.6988	-59.8006

Also, our simulations show that the persons on motion provide additionally shadowing, which the magnitude best fitted by Nakagami as depicted on Figs. 16 and 17.

1) Level Crossing Rate (LCR): Second order statistics are expressed as the level crossing rate (LCR), defined as the rate

at which the envelope crosses a specified level in a positive going direction, and the average fade duration (AFD), the average time for which the received envelope is below that specified level. This measurement of the frequency of fading if the fixed level represents the sensitivity of the receiver.

The LCR allows estimating the average durations of fading in order to determine the code detecting and correct channel error most suitable. To evaluate the LCR we carried out three recordings of amplitude of the signal with 03, 07, 10 and 20 bodies moving in the simulated propagation environment

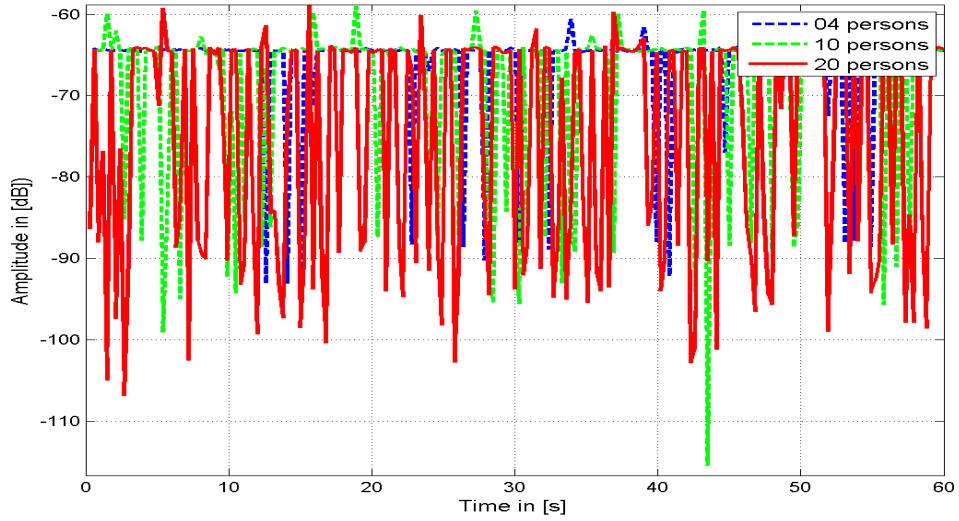


Figure 14. Amplitude variations for 04, 10 and 20 persons.

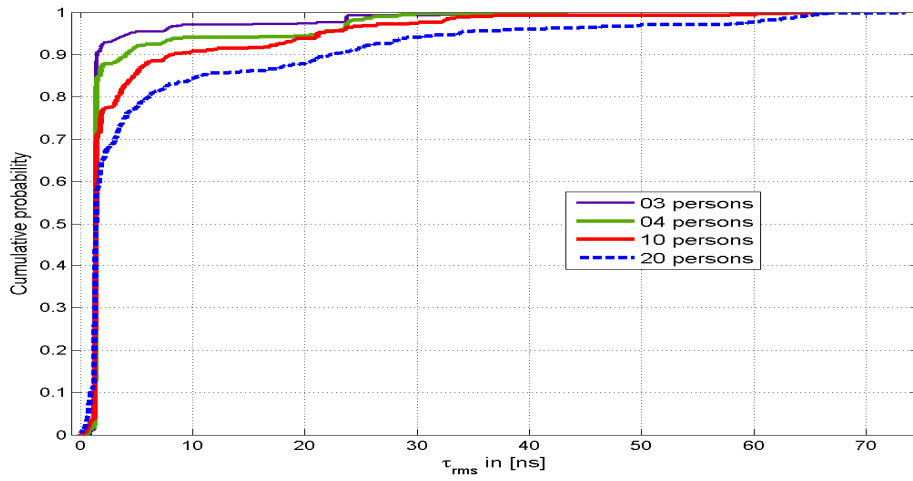


Figure 15.  $\tau_{rms}$  variations for 03, 04, 10 and 20 persons.

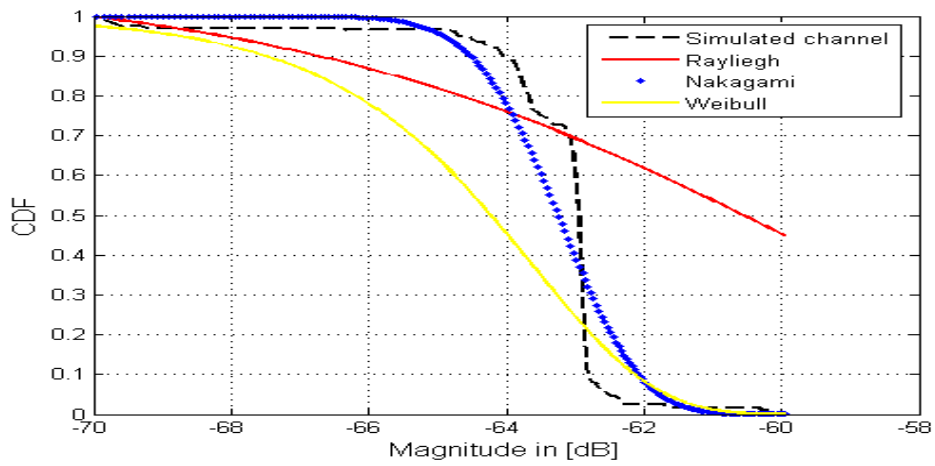
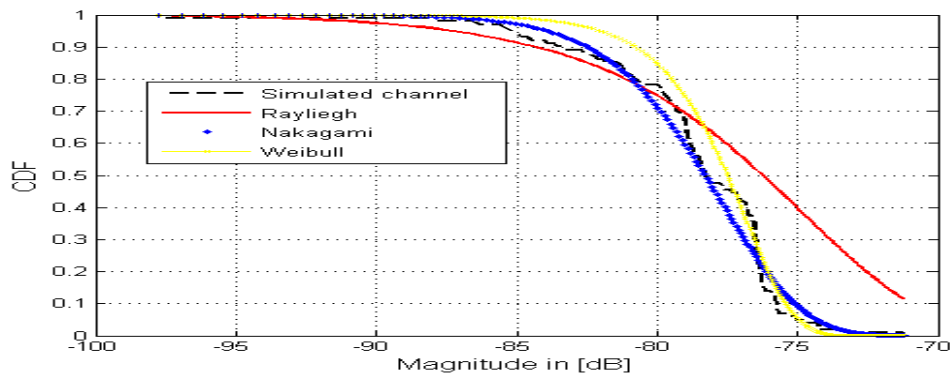


Figure 16. Distribution of the magnitude of direct paths for 04 persons.



**Figure. 17.** Distribution of the magnitude of direct paths for 20 persons.

described above. The LCR is calculated for thresholds varying from the maximum to the minimum of the relative received for different number of persons. Compared to the average value of amplitude of the signal and a distance transmitter-receiver up to 7 m.

Fig. 18 shows that, as the number of peoples within the measurement area increased, the maximum LCR also increased.

This indicates that, as the number of moving peoples within the simulation area increases, the variations in the received envelope also tend to increase.

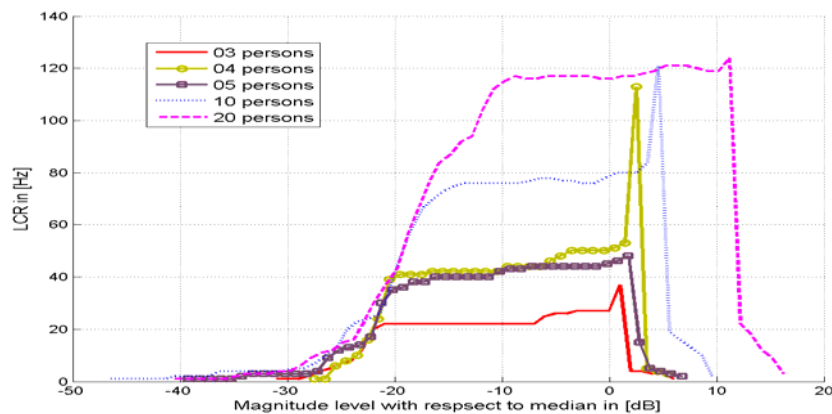


**Figure. 18.** Level Crossing Rate for different number of person in environment.

presents the best fit of simulated channel for different number of persons. The estimated  $m$ -Nakagami parameter is  $m = 12.2635$ ,  $m = 7.1781$ ,  $m = 7.1586$ ,  $2.7592$  and  $m = 1.0326$  for 03, 04, 07, 10 and 20 persons respectively. The Nakagami distribution is defined starting from two parameters,  $m$  and  $\Omega$ .

## 10. Conclusion

In this work, we have presented the simulation results of UWB indoor radio propagation channel. The simulations are performed using a tool that we have developed using RTT and simulated model of human body. First, we have compared UWB channel properties based on simulations and measurements for static environment. The results show that simulations are in agreement with measurements except some fluctuations; these because the simulation does not take in count all features of real environment. In second phase we have performed simulation of channel in dynamic environment.

2) Average Fade Duration analysis: Fig. 19 illustrates the behavior of spectral envelop of relative signal versus the number of people in the environment. From this figure we observe that the bandwidth increase with the number of people.

The analysis of the AFD shows that if the number of people increases the AFD increases that means that the channel become unavailable.

The obtained results confirm the impact of bodies on the propagation. Our results are in agreement with those based on channel measurements, because we have obtained a correlation between channel behavior and number of people in environment. The temporal channel variations become fast if the number of people increases, this is based on analysis of  $\sigma_{rms}$ , LCR and magnitude behaviors. We have observed that the Nakagami distribution presents the best fit of simulated channel, this distribution tends to Rayleigh when the number of peoples increases  $m=1$ , similar result is given in [34]. Finally, this work presents characterization and modeling of a set of channel parameter and show that the RTT can be used to characterize the channel of propagation in a given environment with very knowledge of propagation parameters.

## References

- [1] C. Libe, P. Combeau, A. Gaugue, "Ultra-Wideband Indoor Channel Modelling Using Ray-Tracing Software for through-the-Wall Imaging Radar," *International Journal of Antennas and Propagation*, vol. 2010, Article ID 934602, 14 pages, 2010. doi:10.1155/2010/934602.
- [2] Z. Mohammadi, R. Saadane, D. Aboutajdine, "Ultra Wide-Band Channel Characterization Using Generalized Gamma Distributions," *LNCS Springer Image and Signal Processing*, , 175 \_ 182, 2012.
- [3] Scholtz, R. A. , "Multiple Access with Time-hopping Impulse Modulation," *IEEE Military Communications Conference*, Vol. 2, 11-14 Oct. 1993, pp. 447-450.
- [4] Win, M. Z. , Scholtz, R. A. , "Impulse radio: how it works," *IEEE Communications Letters*, Vol. 2 Issue: 2, Feb. 1998; pp. 36-38.
- [5] R. Saadane, A. Menouni, R. Knopp, and D. Aboutajdine. Empirical eigenanalysis of indoor UWB propagation channels. In *IEEE Globecom*, volume 5, pages 3215 \_ 3219, Nov.-Dec. 2004.
- [6] H Chaibi, R Saadane, M Faqih, M Belkasm, "Spatial Correlation Characterization for UWB Indoor Channel Based on Measurements", *Springer Image and Signal Processing*, 149 \_ 156, 2012.
- [7] R. C. Qiu, "A Study of the Ultra-Wideband Wireless Propagation Channel and Optimum UWB Receiver Design," *IEEE Journal on Selected Area in Communications*, Vol. 20, No: 9, December 2002.
- [8] <http://grouper.ieee.org>.
- [9] A. Saleh and R. Valenzuela, "A statistical model for indoor multipath propagation," *IEEE J. Select. Areas Commun.*, vol. 5, pp. 128-137, Feb. 1987.
- [10] A. Kajiwar, "Indoor propagation measurements at 94 GHz." *Personal, Indoor and Mobile Radio Communications*, 1995. PIMRCapos 95. Apos Wireless: Merging onto the Information Superhighwayapos," *Sixth IEEE International Symposium on Volume 3, Issue* , 27-29 Sep 1995 Page(s): 1026.
- [11] A. Kajiwar, "Millimeter-wave indoor radio channel with artificial reflector", *Vehicular Technology, IEEE Transactions on Volume 46, Issue 2, May 1997* Page(s): 486 - 493.
- [12] Hashemi " The Indoor Radio Propagation Channel " *Proceedings of the IEEE*, Vol.81, No.7, pp. 941-968, July 1993.
- [13] G. L. Turin et al., " A Statistical Model of Urban Multipath Propagation " *IEEE Transactions on Vehicular Technology*, Vol. VT-21, pp. 1-9, February 1972.
- [14] H. Suzuki. " A Statistical Model for Urban Radio Propagation " *IEEE Transactions on Communications*, Vol. COM28, No. 7, pp. 673-680, July 1977.
- [15] H. Hashemi, " Simulation of the Urban Radio Propagation Channel " *IEEE Transactions on Vehicular Technology*, Vol. VT-28, pp.213-224, August 1997.
- [16] John W. McKown an R. Lee Hamilton, Jr. " Ray Tracing as a Design Tool for Radio Networks " *IEEE Network Magazine*, pp. 27-30, November 1991.
- [17] A. Falsafi, K. Pahlavan, G. Yang " Transmission Techniques for Radio LAN's - A Comparative Performance Evaluation Using Ray Tracing " *IEEE Journal on Selected Areas in Communications*, Vol. 14, NO.3, April 1996, pp.477-491.
- [18] P.F.M. Smulders " Geometrical Optics Model For Millimetre Wave Indoor Radio Propagation " *Electronics Letters* 24th June 1993, Vol. 29 No.13, pp.1174-1175.
- [19] G.Yang, K. Pahlavant, J.F. Lee, A.J.Dagent, and J.Vancraeynest " Prediction of Radio Wave Propagation in Four Blocks of New York City Using 3D Ray Tracing " *Proceedings IEEE Conference PIMRC '94*, pp. 263-267.
- [20] P. Kreuzgruber, P. Unterberger, R. Gahleitner "A Ray Splitting Model for Indoor Radio Propagation Associated with Complex Geometries" *Proceedings of 43rd IEEE, Vehicular Technology Conference*, pp.227- 230, May 1993.
- [21] Gargin, D.J., "A fast and reliable acquisition scheme for detecting ultra wide-band impulse radio signals in the presence of multi-path and multiple access interference" *2004 International Workshop on Ultra Wideband Systems*, pp. 106 - 110, May 2004.
- [22] Y. S. Chen , C. C Chiu , C. H Huang, C. H Chen, "Impact of Metallic Furniture on UWB Channel Statistical Characteristics by BER", *Proceeding of WASET* , Vol. 12, pp. 244-247. March, 2006.
- [23] J. El Abbadi, "D'veloppement d'un Outil de Caracatrisation et de Modlisation du canal Radio Mobile Indoor bas la Technique Lancer de Rayons", *th'ese de Doctorat, Ecole Mohammadia d'Ingenieurs*, 1979.
- [24] R. Saadane, A. Hayar, D. Aboutajdine, " Ultra Wideband Channel Statistical Characterization in Different Environments", *International Journal on Information and Communication Technologies*, Vol. 1, No. 1-2, January-June 2008, pp. 57-61.
- [25] Skycross UWB Products, <http://www.skycross.com/Products/uwb.asp#>.
- [26] P. Almers, E. Bonek, A. Burr, N. Czink, M. Debbah, V. Degli-Esposti, H. Hofstetter, P. Kyosti, D. Laurenson, G. Matz, A. F. Molisch, C. Oestges, H. Ozelik , "Survey of Channel and Radio Propagation Models for WirelessMIMO Systems", *EURASIP Journal on Wireless Communications and Networking*, Volume 2007, Article ID 19070.
- [27] B. Uguen, E. Plouhinec, Y. Loutanlen, and G. Chassay, "A deterministic ultra wideband channel modeling," in *IEEE Conference on Ultra Wideband Systems and Technologies Digest of Technical Papers*, pp. 1-5, 2002.
- [28] A. Khafaji, R. Saadane, J. El Abbadi, M. Belkasm, A. Farchi, "Impact of human bodies on millimetric bands propagation using ray tracing technique", *Physical and Chemical News journal*, N 50, pages: 22-31 November 2008.
- [29] A. M. Attiya and A. Safaai-Jazi, "Simlation of ultra-wideband indoor propagation," *Microwvae and optical technology letters*, pp. 103-107, 2004.
- [30] [30] G. A. Schiavone, P. Vahid, R. Palaniappan, J. Trace, and T. Dere, "Analysis of ultra-wide band signal propagation in an indoor environment," *Microwave and Optical Technology Letters*, vol. 36, pp. 13-15, 2003.
- [31] A. Domazetovic, L. J. Greenstein, N. B. Mandayam, and I. Seskar, "A new modeling approach for wireless channels with predictable path geometries," in *Proc. VTC 2003 fall*, pp. 454-458, 2003.
- [32] Z. Mohammadi, R. Saadane, D. Aboutajdine, "Improving the Estimation of the Degrees of Freedom for UWB Channel using Wavelet-Based Denoising," *European Journal of Scientific Research*, 79 (4), 577-591, July, 2012.
- [33] C. Balanis, *Advanced Engineering Electromagnetics*, John Wiley & Sons, New York, NY, USA, 1999.
- [34] P. Pagani, "Caractrisation et modlisation du canal de propagation radio en contexte Ultra Large Bande," *Ph.D. dissertation (in French)*, Institut National des Sciences Appliques de Rennes, France, Nov. 2005.
- [35] M. Ghavami, L. B. Michael R. Kohno, Chapter 4 "UWB CHANNEL MODELING" in the book *Ultra Wideband Signals and Systems in Communication Engineering*, Second Edition, John Wiley and Sons, Ltd, 2007.